

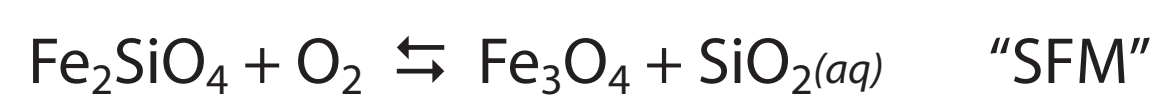
ABSTRACT

Abiotic methanogenesis during metamorphism of ultramafic rocks involving a CO₂-bearing fluid may have played an important role in the evolution of Earth's prebiotic atmosphere. Although many studies focus on the role of oceanic hydrothermal systems, abiotic methanogenesis would likely have accompanied metamorphic fluid-rock interaction in olivine-rich rocks in many Archean crustal environments, including contact, low-grade regional, and subduction-zone metamorphism. To evaluate quantitatively the conditions and productivity of abiotic methanogenesis, we present a series of P-T diagrams contoured for fO₂ and fluid composition. We employ an equilibrium thermodynamic model in which fO₂ is buffered by Fe-bearing olivine, magnetite, and a hydrous ultramafic silicate. We assume ideal solution in all Fe+Mg bearing phases. Our results suggest that serpentinization stabilizes methane-dominant fluids at all calculated pressures (0.25-5 kbar) to roughly 50 °C higher than the forsterite+water = antigorite+brucite equilibrium. For a C-bearing fluid on an Archean oceanic geotherm, this leads to a "metamorphic methane window" of 300-350 °C at ~1 kbar. Once formed, methane is effectively inert, and can be quantitatively degassed to the atmosphere. Given the common occurrence of komatiites in the Archean, their contact and regional metamorphism may have provided important source for atmospheric methane. Similarly, Archean subduction would lead to abiotic methanogenesis in the shallow mantle. Because of the comparatively large volume of ultramafic material in the crust and mantle, its metamorphism could be a larger methane source than methanogenesis by microbes or oceanic hydrothermal systems.

THERMODYNAMIC MODELING

Serpentinization is an fO₂-buffering process, creating redox conditions at low metamorphic grades that are commonly below QFM and occasionally below even IM (Frost, 1984). Figure 1 allows comparison of QFM and IM with the olivine buffers derived in this study.

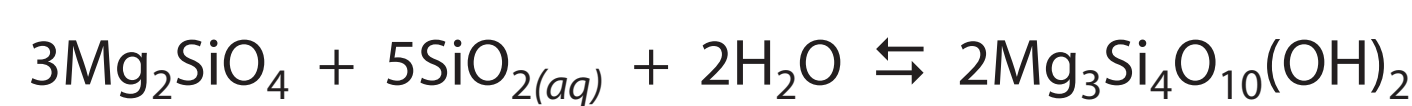
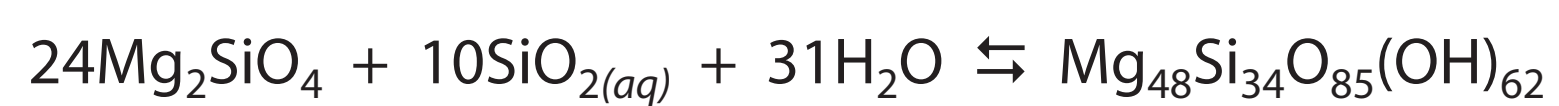
In the presence of magnetite, the fayalite component of olivine and SiO_{2(aq)} buffer fO₂ via:



for which the equilibrium constant is:

$$K_{\text{SFM}} = \frac{(X_{\text{Fa}}^2)^3 f_{\text{O}_2}}{a_{\text{SiO}_2(\text{aq})}^3}$$

At greenschist grade, minerals produced by the serpentinization of olivine include antigorite or talc in equilibrium with fluid, for which the following equilibria can be written:



for which the equilibrium constants are:

$$K_1 = \frac{X_{\text{Atg}}^{48}}{(X_{\text{Fo}}^2)^{24} a_{\text{SiO}_2(\text{aq})}^{10} f_{\text{H}_2\text{O}}^{31}} \quad \text{and}$$

$$K_2 = \frac{(X_{\text{Fa}}^3)^2}{(X_{\text{Fo}}^3)^3 a_{\text{SiO}_2(\text{aq})}^5 f_{\text{H}_2\text{O}}^2}$$

The above equilibrium expressions can be combined to give the model serpentinite buffers, "olivine-antigorite" (OA) and "olivine-talc" (OT):

$$\log f_{\text{O}_2}(\text{OA}) = \log K_{\text{SFM}} - 6 \log X_{\text{Fa}} - 0.3 (48 \log X_{\text{Fo}} + 31 \log f_{\text{H}_2\text{O}} + \log K_{\text{OA}} - 48 \log X_{\text{Atg}})$$

$$\log f_{\text{O}_2}(\text{OT}) = \log K_{\text{SFM}} - 6 \log X_{\text{Fa}} - 0.6 (6 \log X_{\text{Fo}} + 2 \log f_{\text{H}_2\text{O}} + \log K_{\text{OT}} - 6 \log X_{\text{Tlc}})$$

Univariant lines were calculated by assuming ideal solution in all Mg-bearing phases. Partition coefficients were set to unity, a simplification supported by the insensitivity of logK to small variations in X_{Mg} between high-Mg phases. In the NaCl-bearing system, water activities were calculated from the model of Aranovich and Newton (1996). Figures 2 and 3 show the effects, respectively, of decreasing X_{Mg} and increasing X_{NaCl}.

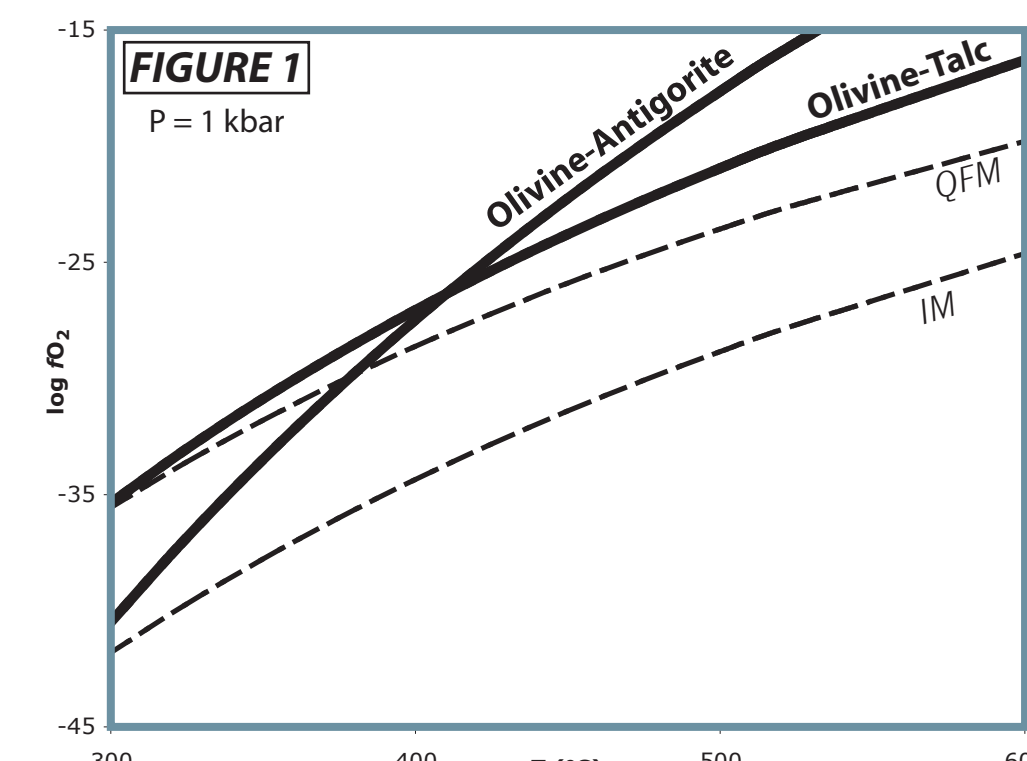


Figure 1: fO₂-T comparison of QFM and IM to the olivine buffers (X_{Fo}=0.9) presented in this study.

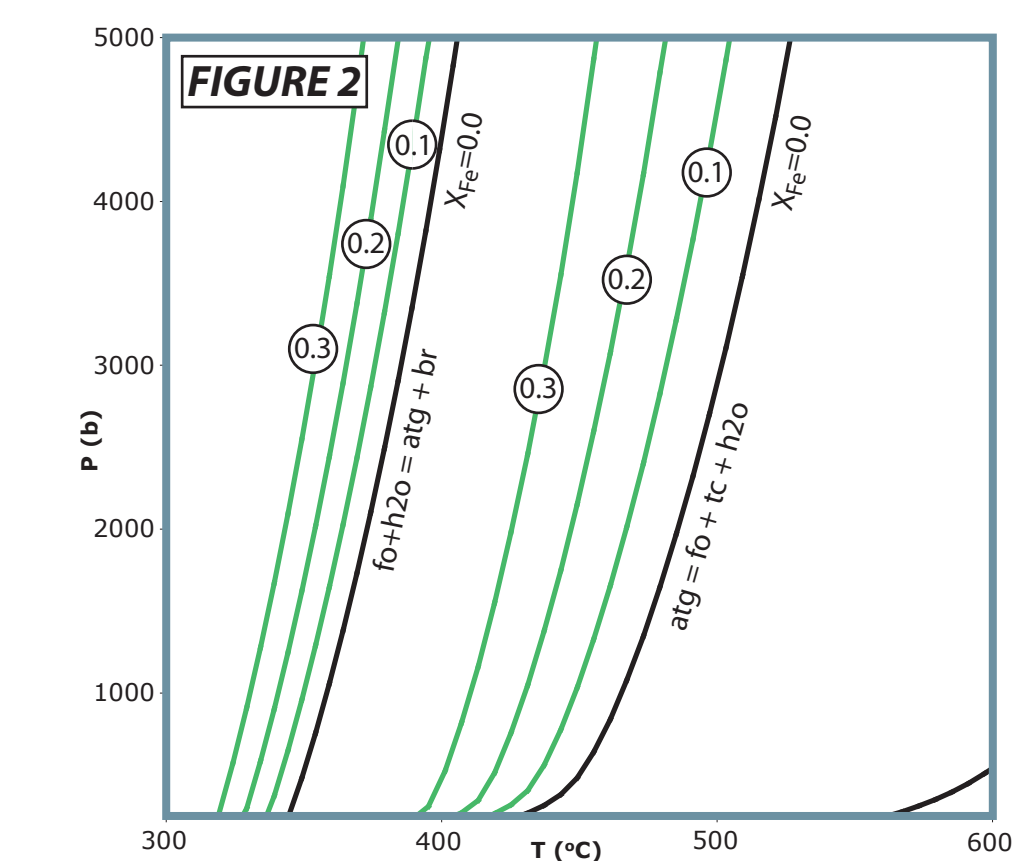


Figure 2: The effect of changing X_{Mg} on the relevant univariant serpentinization equilibria. Solid black lines are pure Mg endmember phases. Circled numbers are X_{Mg}.

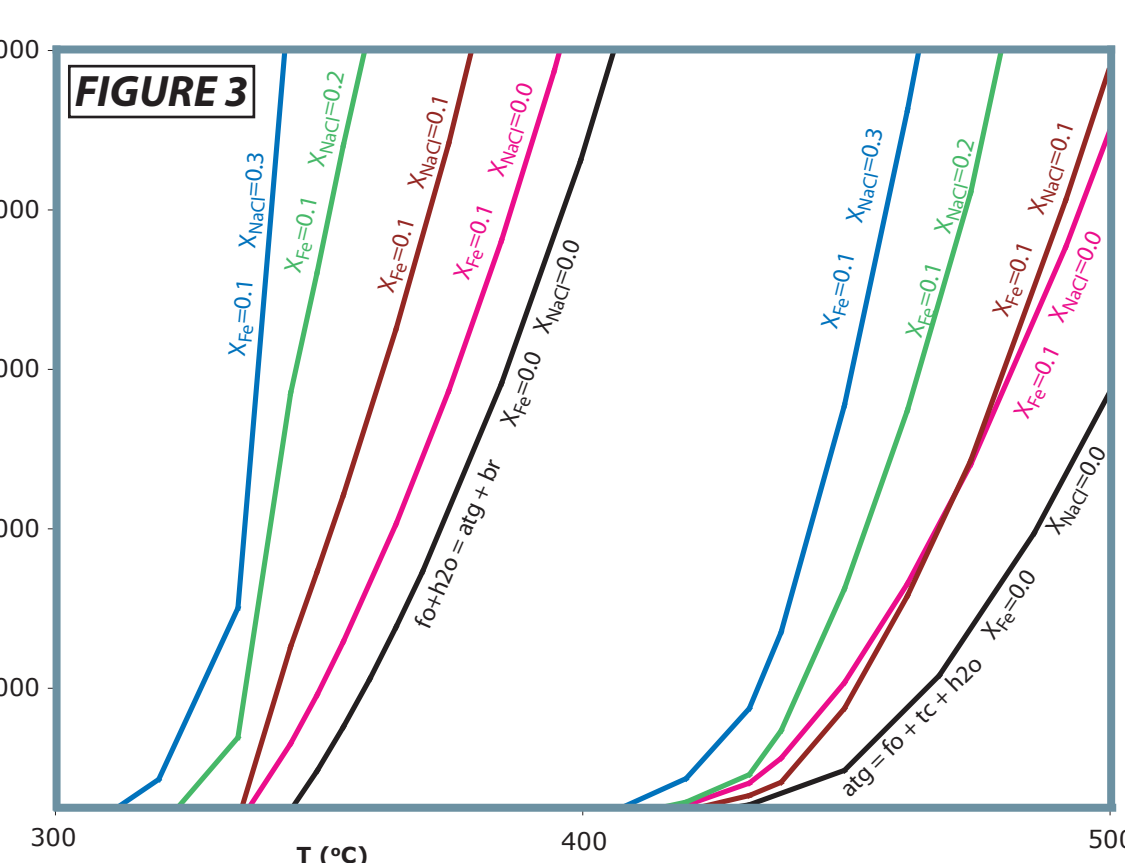


Figure 3: The effect of changing X_{NaCl} on the relevant univariant serpentinization equilibria. Black lines are Fe- and NaCl-free.

In order to compare the redox potential of QFM to the model serpentinite, we plot ΔfO₂ for the olivine buffers in figure 4, where:

$$\Delta f_{\text{O}_2}(\text{OA-QFM}) = \log f_{\text{O}_2}(\text{OA}) - \log f_{\text{O}_2}(\text{QFM})$$

$$\Delta f_{\text{O}_2}(\text{OT-QFM}) = \log f_{\text{O}_2}(\text{OT}) - \log f_{\text{O}_2}(\text{QFM})$$

Negative ΔfO₂ values represent the region of P-T space where the model serpentinite produces more reducing conditions than QFM. The negative ΔfO₂ region in figure 4 is consistent with the P-T region of high fH₂ calculated by Peretti et al (1992). In figure 4, The ΔfO₂ contours are subparallel to the univariant lines. Extrapolation of the zero isoline to higher pressure suggests a field of negative ΔfO₂ that persists to at least several more kbars.

FLUID SPECIATION

Using the fO₂ values calculated from OA and OT, we calculate the bulk speciation of a C-O-H fluid by fixing X_{C,fluid} = 0.1, and solving for log(X_{CH₄/X_{CO₂}), a procedure similar to that published by Lyons et al (2005). When log(X_{CH₄/X_{CO₂}) > 0, methane dominates the carbon component of the fluid. Figure 5 (top right) shows log(X_{CH₄/X_{CO₂}) contours superimposed by two possible shallow P-T paths: an Archean oceanic gradient (Davies, 1992) and a modern hot subduction path (Peacock, 1993). This result suggests both paths could generate methane-dominant fluids. Increasing X_C in the fluid has a weak inverse effect on log(X_{CH₄/X_{CO₂}) and, more importantly, has almost no effect on the P-T location of the boundary between CH₄-rich and CO₂-rich fluids.}}}}

We demonstrate in figure 6 that a low temperature fluid in equilibrium with the model serpentinite is significantly more enriched in methane than a fluid in equilibrium with QFM. For example, a model serpentinite at ~335 °C and 200 bars stabilizes fluids with X_{CH₄/X_{CO₂} values up to ~4 orders of magnitude above QFM. Figure 7 shows %H₂ in the bulk fluid.}

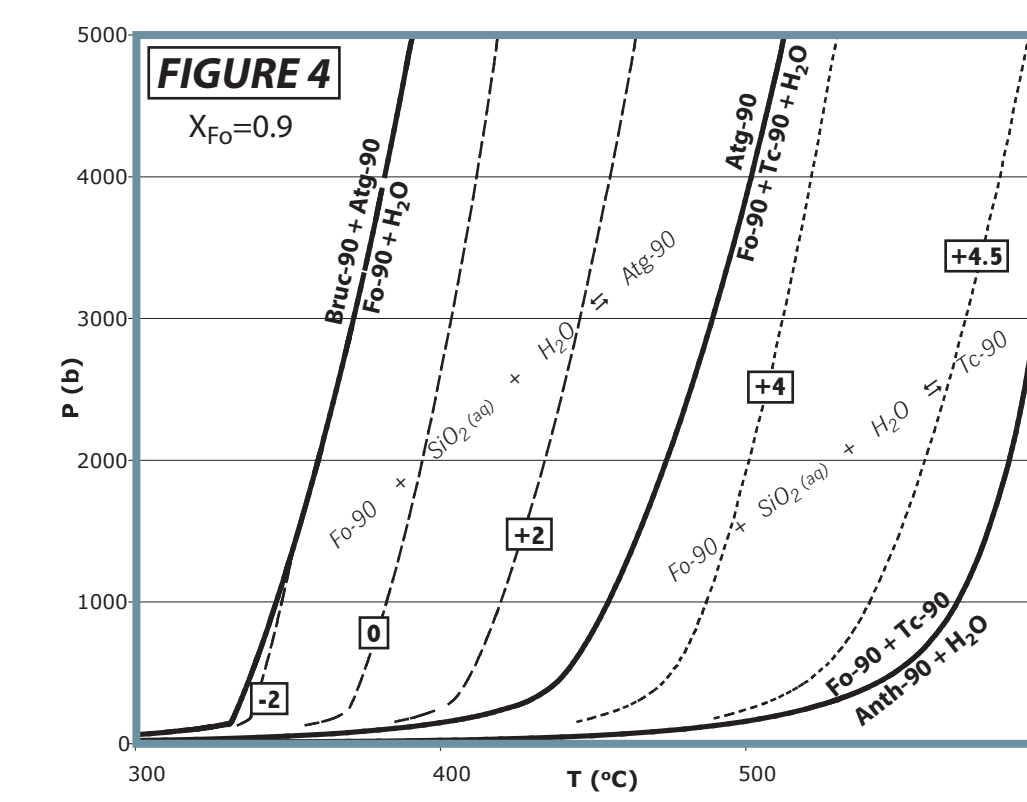


Figure 4: The extent to which OA and OT buffer fO₂ below QFM.

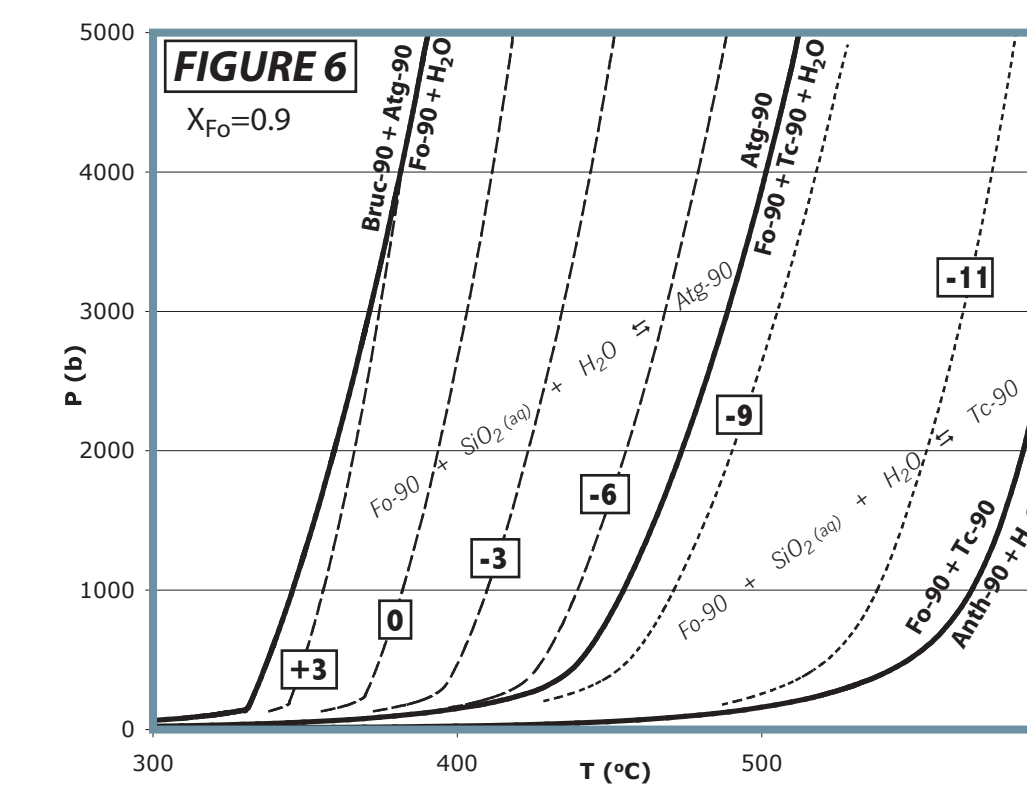


Figure 6: The difference in methane generation between the model serpentinite and QFM. The region to the left of the zero contour represents the P-T space in which the model exceeds the methanogenic potential of QFM.

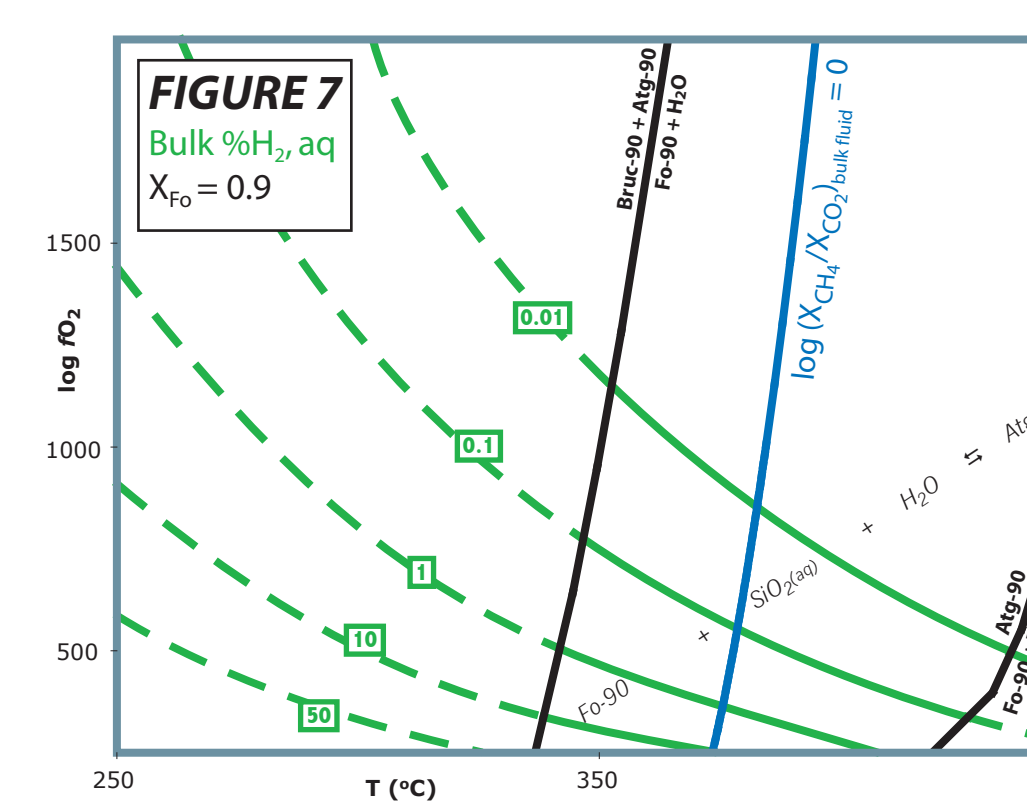


Figure 7: Percent H_{2(aq)} in bulk C-O-H fluid in equilibrium with the model serpentinite. Solid green = equilibrium; dashed = metastable extensions. X_C=0.1 in the bulk COH fluid.

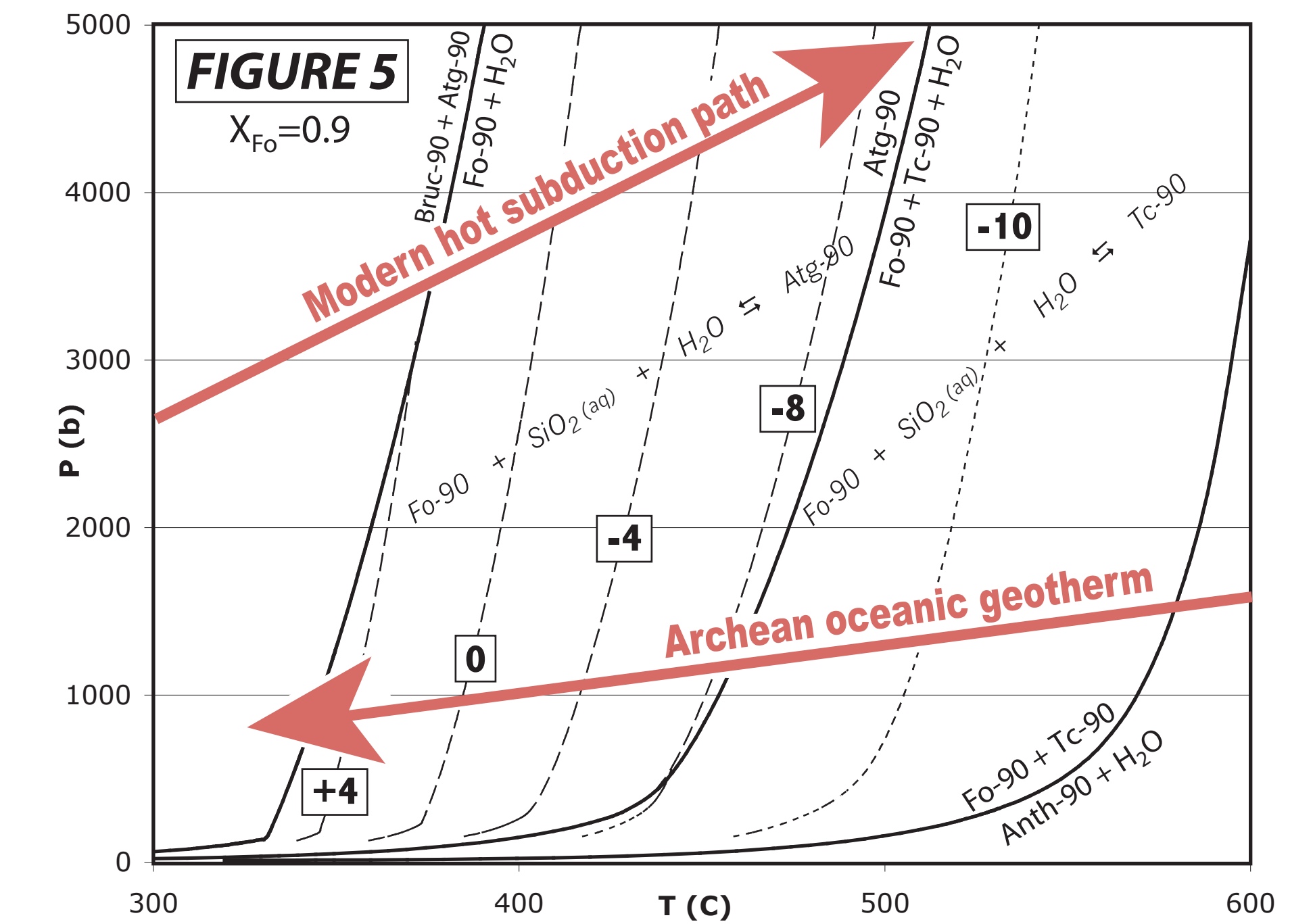


Figure 5: The relative bulk carbon speciation calculated using fO₂ values derived from the OA and OT buffers at X_{C,fluid}=0.1. Methane is the dominant carbon species left of the zero isoline. The superimposition of possible geotherms (Peacock, 1993, Davies, 1992) suggests that serpentinization along shallow P-T paths may stabilize methane-rich fluids, both in the Archean and throughout Earth's history.

VAPOR STABILITY IN A MODEL BRINE

If serpentinization occurs in the presence of a salty solution, then silicate hydration will necessarily lead to a reduction in water activity in the residual fluid by increasing the concentration of dissolved solids. Furthermore, a changing fluid composition will affect liquid-vapor immiscibility. To model these effects, we used GEOFLUIDS (Moller and Weare, 2005) to calculate the limits methane gas stability. Since GEOFLUIDS does not accommodate H₂, we normalized our bulk fluid composition to H₂O-CO₂-CH₄, and varied X_{NaCl} at X_{Mg}=0.9. Figures 8(a-c) demonstrate that increasing X_{NaCl} leads to a larger P-T region of methane gas stability, suggesting that serpentinization by a salty solution will produce methane gas-rich brines.

CONCLUSIONS

In the presence of a C-bearing fluid, abiotic methanogenesis by serpentinization in the Archean is thermodynamically plausible.

Serpentinization can produce methane-rich bulk fluid compositions up to subduction-zone pressures.

Progressive serpentinization by a salty solution can produce progressively more methane vapor-rich brines.

REFERENCES

Aranovich and Newton (1996) *CMP* 125:200-212
 Davies GF (1992) *Geology*, 20: 963:966.
 Frost BR (1985) *Journal of Petrology*, 26: 31-63.
 Kasting JF (2004) *Scientific American*, July: 79-85.
 Lyons JR, Manning CE, Nimmo F (2005) *Geophysical Research Letters*, 32, L13201.
 Moller and Weare (2005) <http://geotherm.ucsd.edu/geofluids/run.html>
 Peacock SM (1993) *GSA Bulletin*, 105: 684-694.

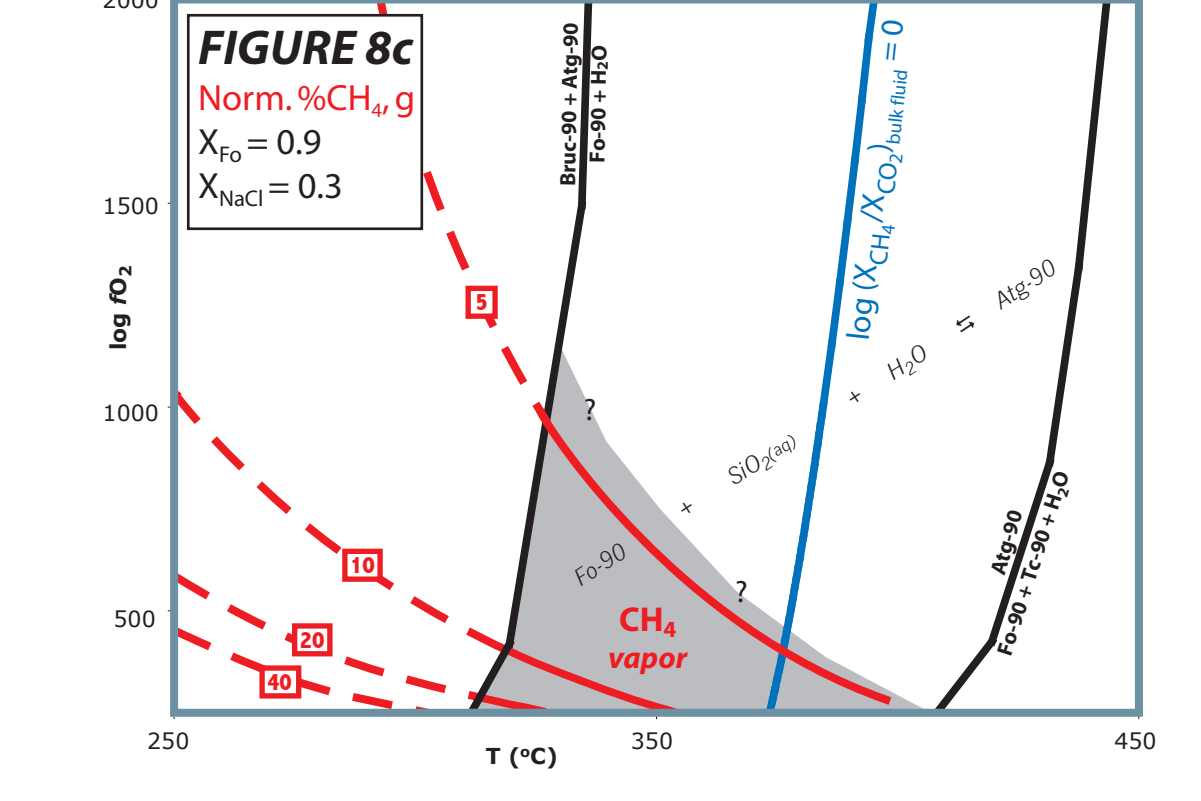
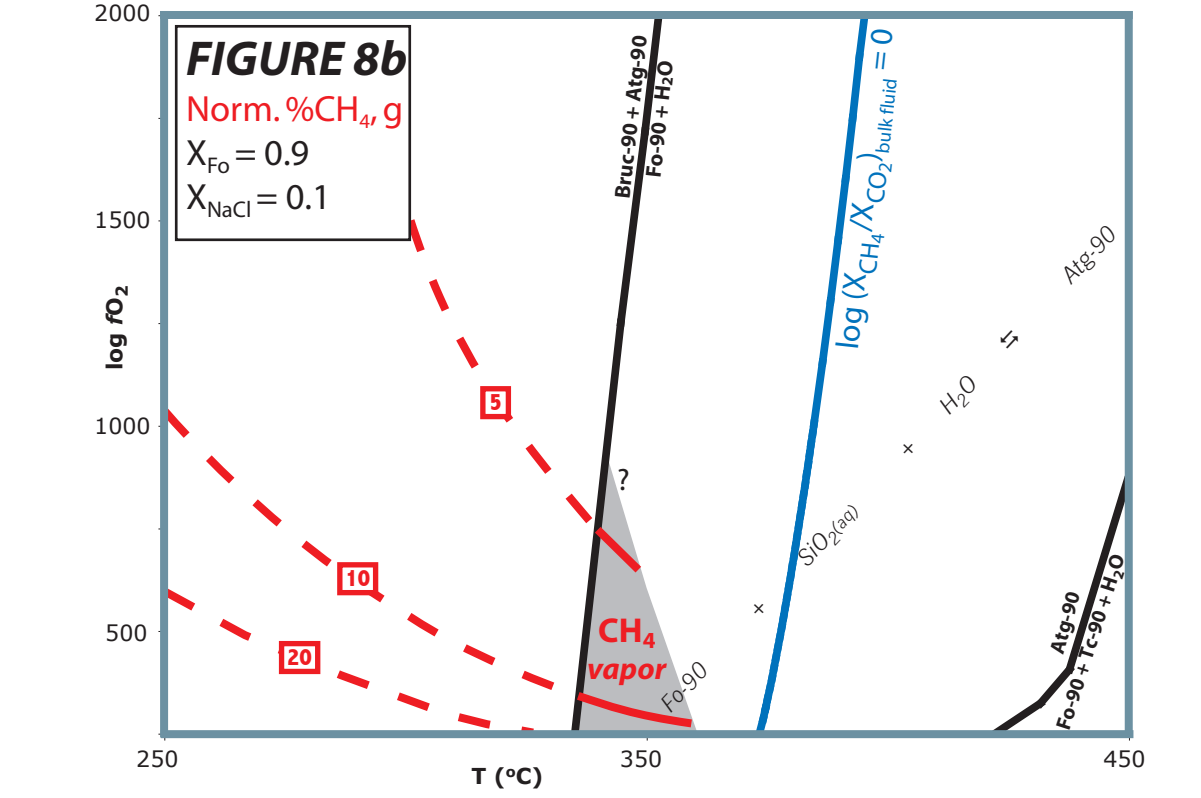
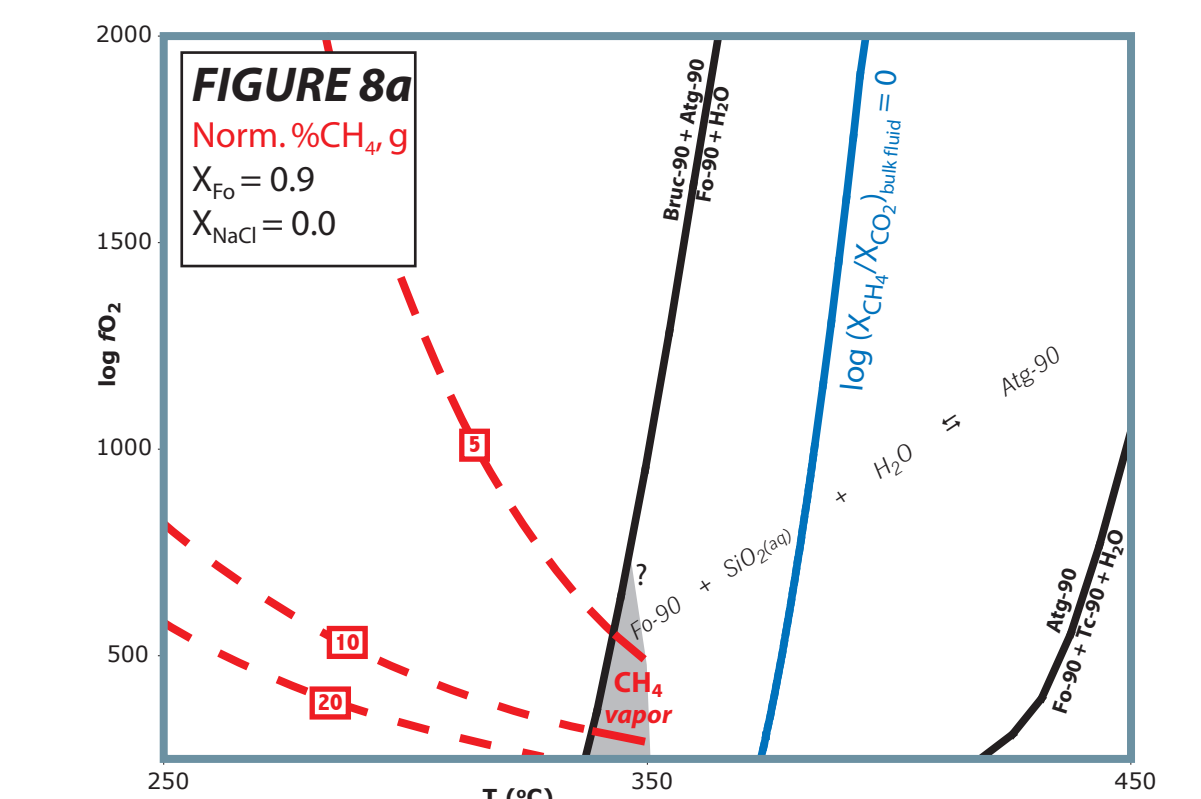


Figure 8: Methane vapor stability in the system H₂O-CH₄-CO₂ in equilibrium with the model serpentinite. Grey region represents vapor immiscibility. Question marks denote extrapolated fields. Red lines represent contours of bulk %CH₄ vapor in a normalized H₂-free fluid. Solid red = equilibrium; dashed = metastable extensions. X_C=0.1 in the bulk C-O-H fluid.